



# Effect of water-retaining lightweight aggregate on the reduction of thermal expansion coefficient in mortar subject to temperature histories

I. Maruyama\*, A. Teramoto

Graduate School of Environmental Studies, Nagoya University, ES-Building, No. 586, Furo-cho, Chikusa-ku, Nagoya 464-8603, Japan

## ARTICLE INFO

### Article history:

Received 22 October 2011

Received in revised form 26 April 2012

Accepted 4 August 2012

Available online 11 August 2012

### Keywords:

Thermal expansion coefficient

Thermal strain

Lightweight aggregate

Internal curing

Autogenous shrinkage

## ABSTRACT

Cement paste containing blast furnace slag with a water to binder ratio of 0.40 showed considerable increase in thermal expansion coefficient due to self-desiccation. Hence the control of thermal expansion coefficient by internal curing with light weight aggregate was studied.

Three types of fine aggregate, hard sandstone, oven-dry light-weight aggregate (LWA) and water-saturated LWA, and three temperature histories were applied to the mortar specimens with a ground granulated blast furnace slag. Total strains and time-dependent thermal expansion coefficients of the mortar specimens were determined using a newly developed setup comprising a specimen temperature regulator and measuring devices for dimensional change of the specimen. As the experiments of total strain and time-dependent thermal expansion coefficient have shown, the water-saturated LWA was able to control the time-dependent thermal expansion coefficient during the temperature history and could be favorably applied to massive concrete undergoing considerable thermal strain. The effectiveness of water-saturated LWA was found to be valid not only for autogenous shrinkage but also for thermal strain produced by the change in thermal expansion coefficient during the temperature history. These strains have been separated from the total strain by the proposed method.

© 2012 Elsevier Ltd. All rights reserved.

## 1. Introduction

The thermal expansion coefficient of cement paste is affected by the relative humidity within the cement paste and increases with a decrease in relative humidity at a relative humidity above 70% [1,2]. Bazant divided the thermal dilatation of cement paste into the thermal expansion of solid and deformation associated with water redistribution inside of the cement paste [3]. The effect of temperature on the relative humidity within cement paste was experimentally studied by Radjy et al. [4], and Grasley and Lange conducted experiments and analysis of the dependence of thermal expansion coefficient on relative humidity that acted as a driving force of shrinkage due to capillary tension [5]. The above studies have clarified to some extent the dependence of thermal expansion coefficient on relative humidity.

When water–binder ratio is relatively low, a decrease in relative humidity in concrete due to self-desiccation at early ages was observed associated with the development of hydration reactions. This also resulted in an increase in thermal expansion coefficient [6].

The time-dependent thermal expansion coefficient of OPC and BFS cement pastes with water–binder ratios of 0.4 and 0.55 were

determined by the authors under constant temperature of 20 °C and elevated temperature histories [7]. It was shown that the thermal expansion coefficient of the OPC cement paste with a water cement ratio of 0.4 and BFS cement paste with a water–binder ratio of 0.40 and 0.55 increased with the development of hydration and the increase was accelerated when the elevated temperature was higher. This implied that the increase in thermal expansion coefficient due to self-desiccation, reported by Bjontegaard et al., might also be present at the region of relatively high water–binder ratios, and that, when subjected to elevated temperature histories, the increase in thermal expansion coefficient (which was larger at descent rather than at ascent) resulted in the presence of the residual shrinkage strain after the specimen temperature became constant.

The shrinkage strain originating from the time-dependent thermal expansion coefficient could be a cause of thermal cracking of massive concrete hence its preventive measures need to be developed. Internal curing is a measure to control the thermal expansion coefficient by which this study proposed a new method of maintaining a high relative humidity within the cement paste. Aggregate with high moisture content has often been used for controlling autogenous shrinkage strain [8]. Numerous test results of autogenous shrinkage strain under various constant temperatures have been reported, while little is known about the use of internal curing to control the autogenous shrinkage and the

\* Corresponding author. Tel.: +81 52 789 3761; fax: +81 52 789 3773.

E-mail address: [ippei@dali.nuac.nagoya-u.ac.jp](mailto:ippei@dali.nuac.nagoya-u.ac.jp) (I. Maruyama).

**Table 1**  
Properties of Portland cement.

|     | Density (g/cm <sup>3</sup> ) | Blaine value (cm <sup>2</sup> /g) | LOI (%) | Chemical composition (% mass) |                                |                                |      |      |                 |                   |                  |                 |
|-----|------------------------------|-----------------------------------|---------|-------------------------------|--------------------------------|--------------------------------|------|------|-----------------|-------------------|------------------|-----------------|
|     |                              |                                   |         | SiO <sub>2</sub>              | Al <sub>2</sub> O <sub>3</sub> | Fe <sub>2</sub> O <sub>3</sub> | CaO  | MgO  | SO <sub>3</sub> | Na <sub>2</sub> O | K <sub>2</sub> O | Cl <sup>−</sup> |
| OPC | 3.16                         | 3110                              | 0.64    | 21.8                          | 4.49                           | 2.90                           | 63.9 | 1.84 | 2.26            | 0.20              | 0.38             | 0.007           |

**Table 2**  
Properties of blast furnace slag.

|       |      | Density (g/cm <sup>3</sup> ) | Blaine value (cm <sup>2</sup> /g) | LOI (%) | Chemical composition (% mass) |                                |       |      |      |      |                   |                  |                  |       |
|-------|------|------------------------------|-----------------------------------|---------|-------------------------------|--------------------------------|-------|------|------|------|-------------------|------------------|------------------|-------|
|       |      |                              |                                   |         | SiO <sub>2</sub>              | Al <sub>2</sub> O <sub>3</sub> | FeO   | CaO  | MgO  | S    | Na <sub>2</sub> O | K <sub>2</sub> O | TiO <sub>2</sub> | MnO   |
| GGBFS | 2.90 | 4050                         | 0.05                              | 33.88   | 15.34                         | 0.34                           | 42.65 | 5.81 | 0.65 | 0.28 | 0.31              | 0.57             | 0.16             | 0.004 |

**Table 3**  
Physical property of fine aggregate.

| Materials               | Type                  | Character   |
|-------------------------|-----------------------|---|
| Fine aggregate: agg-N   | Crushed sand          | Surface dry density: 2.57 g/cm <sup>3</sup> , water absorption: 2.62% |
| Fine aggregate: agg-LWA | Lightweight aggregate | Surface dry density: 1.86 g/cm <sup>3</sup> , water absorption: 18.8% |

increase in thermal expansion coefficient during temperature histories.

The target material in this study is blast furnace slag (BFS) cement mortar with a water–binder ratio of 0.4. Previous research has shown that the BFS cement is sensitive to the increase in thermal expansion coefficient due to self-desiccation [7] and the BFS cement mortar should undergo larger volume changes at early stages than those of ordinary mortar, with reference to past experiments showing larger autogenous shrinkage strain [9] and thermal expansion coefficient [10] of BFS concrete than those of ordinary concrete.

## 2. Experimental program

### 2.1. Materials

Binder types used in this experiments were ordinary Portland cement (OPC), ground granulated blast furnace slag (GGBFS) and anhydrite with a specific surface area of 4690 cm<sup>2</sup>/g. Properties of the OPC and GGBFS are shown respectively in Tables 1 and 2. The binder compound used in this experiment was OPC substituted by 30% with a secondary binder compound comprising GGBFS substituted by 3.4% with anhydrite. The water to powder ratio was 0.40.

Mortar specimens were prepared with three types of fine aggregates: a crushed hard sandstone (agg-N), a shale-based LWA with a saturated surface-dry moisture condition (agg-LWA-S) and the shale-based LWA with oven-dry moisture condition (agg-LWA-D). The physical properties of aggregates are listed in Table 3. Three types of mortar with an aggregate content of 38% by volume were produced, where single use of agg-N (38%), agg-N (19%) plus agg-LWA-S (19%) and agg-N (19%) plus agg-LWA-D (19%) were applied. These mortar specimens are denoted as N, LWA-S, and LWA-D respectively.

Before mixing, materials were kept for 24 h in a thermostatic chamber at a temperature of 20 °C. Mixing of 20 l per batch was performed with the Omni mixer at room temperature of 23 °C. After introducing water and a mixing of 3 min, scraping was performed followed by a mixing of another 3 min. Then the fresh mortars were moved to the thermostatic chamber. The point of zero age for all data is the time when the powder materials are first mixed with water.

Fine aggregates were conditioned to have a saturated surface-dry moisture content. They were first vacuum-saturated and kept under water for a week. The day before the experiment, they were subjected to a blow drying associated with a repeated confirmation of the saturated surface-dry moisture content by the ASTM C127 cone method. The conditioned aggregates were sealed with a plastic bag and stored until weighing.

### 2.2. Temperature history

Three temperature histories were applied to the specimen, namely 20 °C–constant (denoted as –20), elevated up to 40 °C (denoted as –40) and elevated up to 60 °C (denoted as –60). The latter two were meant to simulate the hydration heat-induced temperature history in concrete such that, as shown in Fig. 1, keeping 20 °C for the first 10 h and increasing up to the maximum temperature from 10 to 22 h with a rate of temperature increase of 3.33 °C/h (in the case of max. 60 °C) and 1.67 °C/h (in the case of max. 40 °C). After reaching the maximum temperatures, they were kept for 10 h (from 22 to 32 h), after which temperatures were decreased to reach 20 °C at the age of 144 h. The rates of temperature decrease were 0.357 °C/h (in the case of max. 60 °C) and 0.179 °C/h (in the case of max. 40 °C).

Simultaneously with the above temperature histories, short thermal pulses were applied to the specimens to determine the thermal expansion coefficient at each material age. The thermal pulse was plus and minus 5 °C with a rate of 0.2 °C/min and applied every 340 min for the specimen kept under the constant temperature of 20 °C and, for the specimens subjected to a maximum temperature of 60 and 40 °C, at ages of 7, 13, 18, 23, 28, 33, 52, 77, 102, 127, 152, 159, 166 h. Typical temperature change profiles with thermal pulses are shown in Fig. 1. These temperature histories were determined based on the numerical results of a thick wall using FEM with an experimental adiabatic temperature rise data as an input [11,12], and on an experimental measurement.

### 2.3. Strain measurement [7]

The length-change measuring apparatus used in the experiments is shown in Fig. 2. Dimensions of the specimen for length-change measurement was 10 × 60 × 370 mm which was thin enough to ensure uniform temperature distribution within ±0.2 °C.

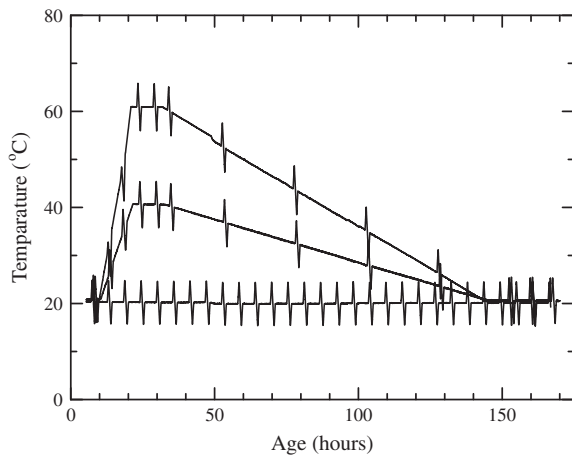


Fig. 1. Applied temperature history.

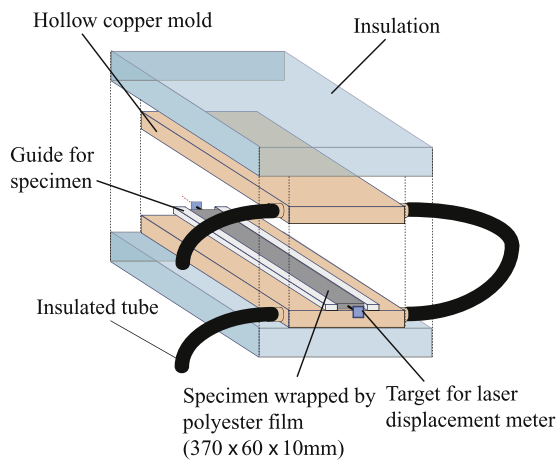


Fig. 2. Schematic of measurement system.

Specimen temperature was controlled by circulating thermostatic water in the hollow copper mold around the specimen using a thermostatic bath (heating capacity of 1.0 kW, cooling capacity of 150 W and flow rate of 15 l/min). The copper mold and the specimen were thermally insulated with a polystyrene foam of 30 mm thick to minimize heat exchange with the room air. Specimens were wrapped with a polyester film with a thickness of 0.05 mm to prevent friction between cement paste and the copper plate and to prevent drying of the specimen.

The longitudinal direction of the specimen was measured with two laser displacement meters at a resolution of 0.5  $\mu\text{m}$ . Thermal expansion coefficient was determined by the strain measurement results. It is an average of slope of strain under a thermal pulse, and based on the measured total strain and calculated thermal expansion coefficient and temperature of specimen, autogenous shrinkage of specimen was obtained.

### 3. Results and discussion

#### 3.1. Total strain

Measured total strains are shown in Figs. 3–5. It is shown that the maximum expansive strains at 60 °C of the specimens with lightweight aggregates, LWA, are larger than that using the hard sandstone only, N. When the expansive strain of LWA-D-60 and LWA-S-60 are 622  $\mu$  and 673  $\mu$ , that of N-60 is as low as 534  $\mu$ . After the age of 150 h, total strains of N-60, LWA-D-60 and LWA-S-60 are

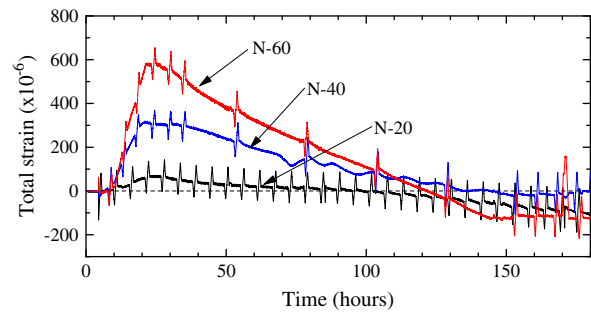


Fig. 3. Total strain of specimen N.

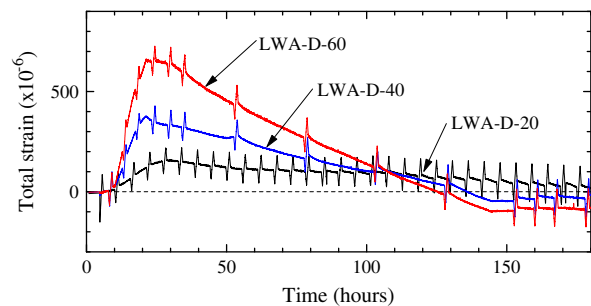


Fig. 4. Total strain of specimen LWA-D.

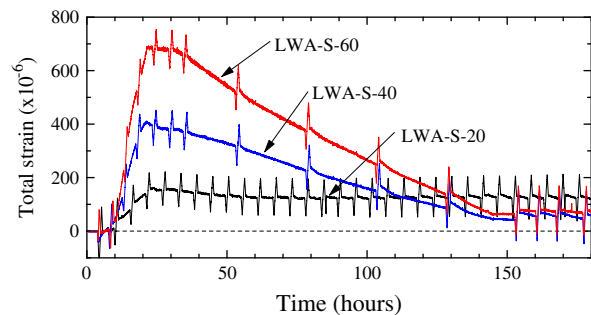


Fig. 5. Total strain of specimen LWA-S.

–124  $\mu$ , –100  $\mu$  and +63  $\mu$  showing a distinctive expansion in LWA-S-60.

To estimate the residual strains after elevated temperature histories, the strain at the maximum temperature and that after the temperature histories at the age of 150 h are compiled in Table 4. Because LWA-S shows an expansive residual strain and the smallest difference from the maximum strain, an internal curing effect of water-retaining lightweight aggregate on the thermal expansion coefficient is unquestionable. The volume change mechanism and impact of LWA will be discussed through separation of thermal strain and autogenous shrinkage in the following chapter.

#### 3.2. Thermal strain and autogenous shrinkage strain

Thermal expansion coefficients obtained from the temperature and total strain measurements are shown in Figs. 6–8. The error bar means the range of thermal expansion coefficients obtained from the ascending and descending temperatures of a thermal pulse.

Compared with the specimen kept at a constant temperature of 20 °C, specimens subjected to elevated temperature histories up to 40 °C and 60 °C show larger thermal expansion coefficient at early stages. This is attributed to an early development of self-desicca-

**Table 4**

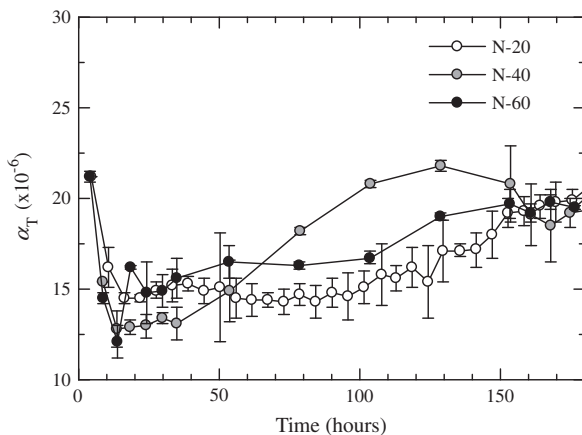
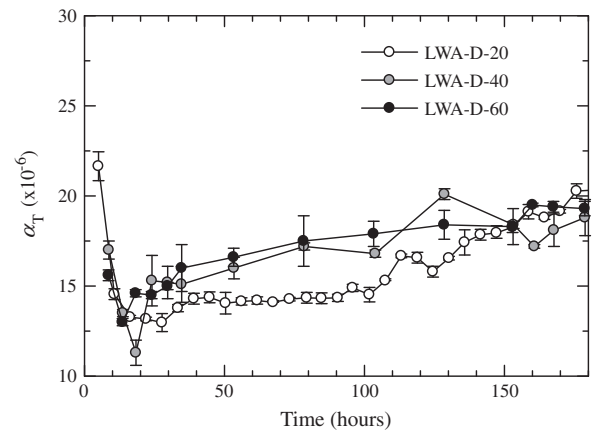
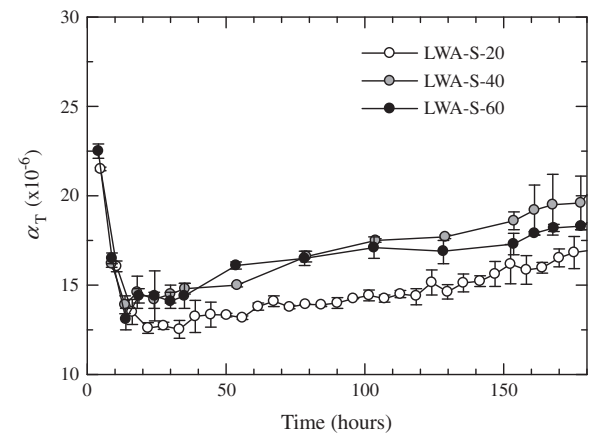
Total strain at the peak temperature, strain after elevated temperature history, and resultant strain under temperature decrease.

|          | Total strain at the peak temp. (18–32 h) ( $\times 10^{-6}$ ) | Total strain at 20 °C. (150 h) ( $\times 10^{-6}$ ) | Difference ( $\times 10^{-6}$ ) |
|----------|---|---|---------------------------------|
| N-60     | 534   | –124  | 658                             |
| LWA-D-60 | 622   | –100  | 721                             |
| LWA-S-60 | 673   | 63  | 610                             |
| N-40     | 311   | 2   | 309                             |
| LWA-D-40 | 358   | –31   | 389                             |
| LWA-S-40 | 397   | 146   | 251                             |

tion by the accelerated hydration. Regardless of the type of aggregate, thermal expansion coefficient of specimens subjected to the elevated temperature history of 40 °C sometimes exceeds those of 60 °C and 20 °C. Mechanisms of the behavior are left for the future study while the temperature dependence of hydrophilicity of hydrates may pose some influence.

Changes in thermal expansion coefficient of specimens subjected to each temperature history are compared in Fig. 9, where the thermal expansion coefficient of LWA-S subjected to the constant temperature of 20 °C obviously increased after 100 h. Also when subjected the temperature history of 40 °C, from 75 to 150 h, thermal expansion coefficient of LWA-S was lower than that of N, 40 °C, from 75 to 150 h, thermal expansion coefficient of LWA-S was lower than that of N.

Using the obtained thermal expansion coefficient, the total strain was separated into thermal and autogenous strains, and resultant calculated autogenous strains are shown in Figs. 10–12. All the specimens showed expansion during the first 24 h after casting, and LWA-S and LWA-D showed expansive peak strain were of approx. 150  $\mu$  while that of N ranged from 50  $\mu$  to 100  $\mu$ . This expansion is attributed to the formation of ettringite because all the ages that gave the peaks were consistent, and the difference in expansive strain is attributed to the difference in the average bulk modulus, in other words, less restraining effect of LWA on the expansion of cement paste is smaller. LWA also showed expansion during drying process [13], for which another explanation may be needed. Regarding the autogenous shrinkage, after initial expansion during the first 20 h, the autogenous shrinkage of specimens subjected to an elevated temperature history exhibit a local minimum value at the age of 50–100 h followed by a gradual expansion, while regardless of the temperature history, specimens with LWA showed similar autogenous shrinkage behavior and are always on the expansive side. The expansive strain of LWA-S is larger than that of LWA-D showing an effect of internal curing on the autogenous shrinkage.

**Fig. 6.** Thermal expansion coefficients of specimen N.**Fig. 7.** Thermal expansion coefficients of specimen LWA-D.**Fig. 8.** Thermal expansion coefficients of specimen LWA-S.

Among N specimens, continuous autogenous shrinkage was found only in those kept under constant temperature, while the other specimens showed slightly expansive tendency. On the other hand, the total strain of the specimens subjected to elevated temperature history exhibit considerable shrinkage that can be attributed to the thermal strain as shown in Table 4.

Separation of the total strain into thermal and autogenous strains was based on the consecutive measurement of thermal expansion coefficient using a short thermal pulse of 100 min in length. Because there are many unknown factors regarding the thermal expansion coefficient of hardened cement paste, such as delayed expansion [14], the separation of the total strain performed in this study is not always in the general agreement.

It was also reported that autogenous shrinkage at high temperatures was even small when the temperature was kept constant [15]. Assuming this is originated from a change in the hydration products by temperature, gradual increase in the expansive strain under temperature changes, as shown in our experiments, is not improbable.

Finally, contributions of saturated LWA to the strain under the temperature history are summarized in Fig. 13. In this figure, total strain, autogenous shrinkage and thermal strain produced by time-dependent behavior of thermal expansion coefficient of N-60, LWA-D-60, and LWA-S-60 at 7-day are compared. As it is shown in Fig. 13, saturated LWA produce 130  $\mu$ -expansion in autogenous strain and 60  $\mu$ -expansion in thermal strain when LWA-S-60 is compared with N-60. This figure proves that the internal curing contributes to compensating not only the autogenous shrinkage

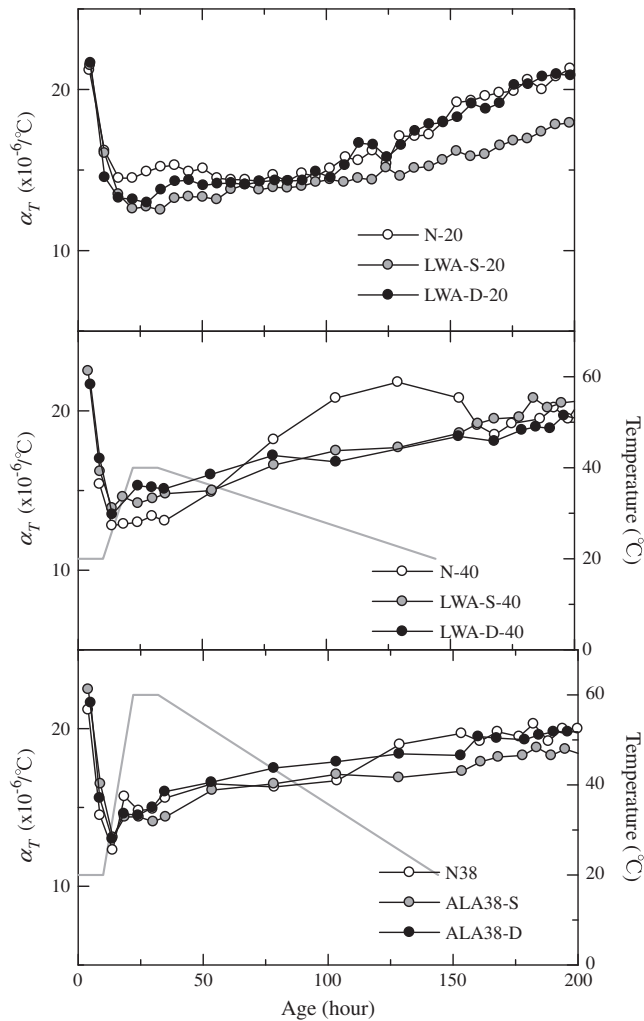


Fig. 9. Comparison of thermal expansion coefficient of N, LWA-D, and LWA-S.

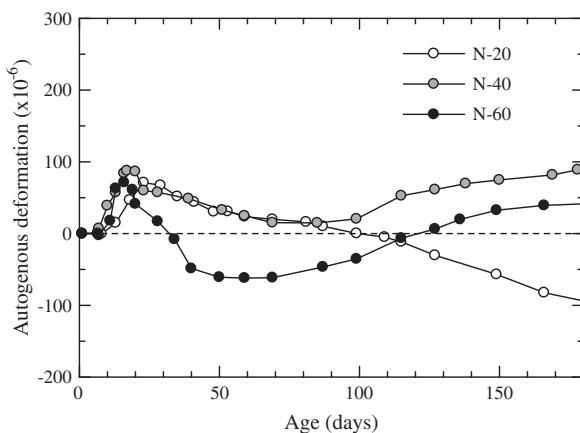


Fig. 10. Autogenous shrinkage of specimen N.

but also the thermal strain due to time-dependent behavior of thermal expansion coefficient.

#### 4. Concluding remarks

Aiming at controlling increase in thermal expansion coefficient due to self-desiccation, three types of fine aggregate (100% hard

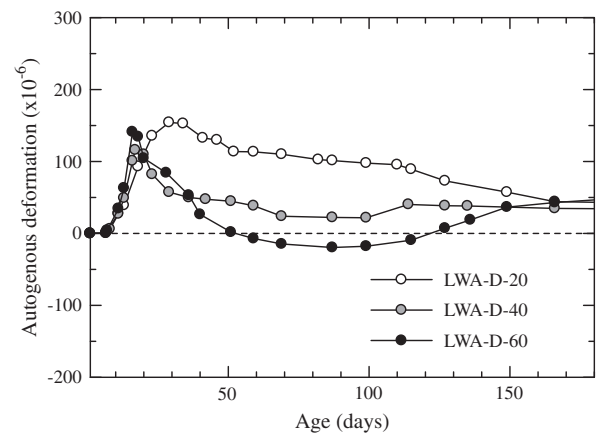


Fig. 11. Autogenous shrinkage of specimen LWA-D.

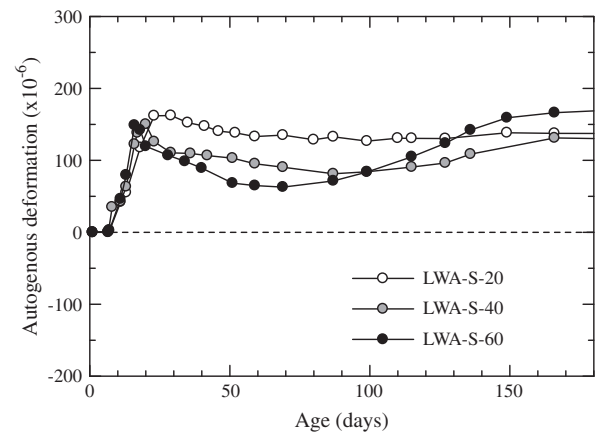


Fig. 12. Autogenous shrinkage of specimen LWA-S.

sandstone (denoted as N), 50% hard sand stone and 50% oven-dry LWA (denoted as LWA-D) and 50% hard sand stone and 50% water-saturated LWA (denoted as LWA-S) were introduced to cement paste with a blast furnace slag. The total strain and the time-dependence of thermal expansion coefficient were determined under temperatures of 20 °C constant and two temperature histories that assumed elevated temperatures due to hydration heat. The following findings were obtained:

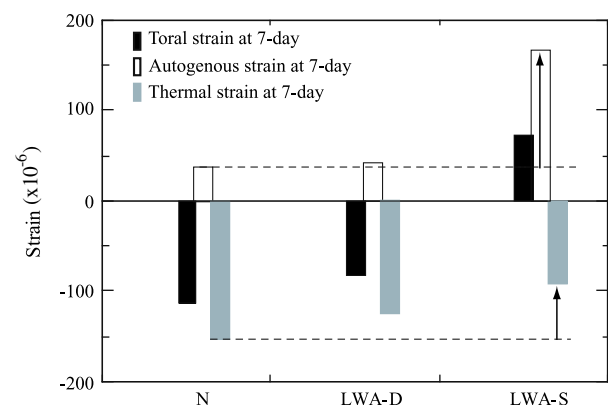


Fig. 13. Comparison of total strain, autogenous shrinkage and thermal strain of N-60, LWA-D-60, and LWA-S-60 at 7-day.

- (1) Among three types of fine aggregates, the time-dependence of thermal expansion coefficient of N and LWA-D showed similar behavior while LWA-S was smaller than those of the others. Taking into account the known fact that drying causes an increase in thermal expansion coefficient, it is concluded that the internal curing effect of water-saturated LWA could control the increase in thermal expansion coefficient.
- (2) In addition to the autogenous shrinkage, a considerable shrinkage strain originated from the dependence of thermal expansion coefficient on the development of hydration and elevated temperature history was confirmed when a mortar with the ordinary Portland cement, the granulated blast furnace slag and sandstone aggregate was subjected to elevated temperature histories due to hydration heat liberation. Calculated thermal strain taking account of the time-dependence of thermal expansion coefficient exceeded the total strain measured after the elevated temperature history, because the autogenous strain was expansive at an elevated temperature history.
- (3) The measured total strain after the elevated temperature history of LWA-D was slightly smaller than that of N. However, the effect of the dependence of thermal expansion coefficient on the development of hydration and elevated temperature history on the total strain was considerable regardless of the type of aggregate.
- (4) The total strain after elevated temperature history of LWA-S was expansive. This can be attributed to the internal curing that has made the autogenous strain largely expansive and that has controlled the increase in thermal expansion coefficient due to self-desiccation, resulting in the reduction of shrinkage strain due to the dependence of thermal expansion coefficient on the development of hydration and to the elevated temperature history.

The above findings imply that the use of water-saturated LWA is preferable for mass concrete members with a large cross section in terms of controlling autogenous shrinkage and increase in thermal expansion coefficient due to the development of hydration.

Appropriate mix design of concrete taking account of strength and fluidity needs to be studied for the practical application of the proposed concept.

### Acknowledgments

This study forms a part of Grant-in-Aid for Young Scientists (A) 21686052 and Grant-in-Aid for Scientific Research (A) 21246071 supported by JSPS, The Ministry of Education, Culture, Sports, Science and Technology of Japan.

### References

- [1] Meyers SL. Thermal expansion characteristics of hardened cement paste and of concrete. *Highway Res Board Proc* 1950;30:193–203.
- [2] Sellevold EJ, Bjøntegaard O. Thermal dilation and internal relative humidity of hardened cement paste. *Mater Struct* 2006;39:809–15.
- [3] Bazant ZP. Delayed thermal dilatations of cement paste and concrete due to mass transport. *Nucl Eng Des* 1970;14:308–18.
- [4] Radjy F, Sellevold EJ, Hansen KK. Isothermic vapor pressure–temperature data for water sorption in hardened cement paste: enthalpy, entropy and sorption isotherms at different temperatures. *Tech Univ of Denmark*; 2003.
- [5] Grasley ZC, Lange DA. Thermal dilation and internal relative humidity of hardened cement paste. *Mater Struct* 2007;40:311–7.
- [6] Bjøntegaard Ø, Sellevold EJ. Interaction between thermal dilation and autogenous deformation in high performance concrete. *Mater Struct* 2001;34:266–72.
- [7] Maruyama I, Teramoto A. Impact of time-dependant thermal expansion coefficient on the early-age volume change in cement pastes. *Cem Concr Res* 2011;41:380–91.
- [8] Kovler K, Jensen OM, editors. Internal curing of concrete. State-of-the-art report of RILEM technical committee 196-ICC, Report 41; 2007.
- [9] Tazawa E, Miyazawa S. Influence of cement and admixture on autogenous shrinkage of cement paste. *Cem Concr Res* 1995;25:281–7.
- [10] Japan Concrete Institute. Guidelines for control of cracking of mass concrete; 2008.
- [11] Architectural Institute of Japan. State of the art report on mass concrete. Maruzen, Tokyo; 2001. p. 124 [in Japanese].
- [12] Japan Concrete Institute. Report of JCI-TC-043A. Control of cracking of mass concrete; 2006. p. 198 [in Japanese].
- [13] Lura P. Autogenous deformation and internal curing of concrete. PhD thesis, Delft University of Technology, The Netherlands; April 2003.
- [14] Sabri S, Illston JM. Immediate and delayed thermal expansion of hardened cement paste. *Cem Concr Res* 1982;122:199–208.
- [15] Lura P, van Breugel K, Maruyama I. Effect of curing temperature and type of cement on early-age shrinkage of high performance concrete. *Cem Concr Res* 2001;31:1867–72.